© 2014. Published by The Company of Biologists Ltd | Development (2014) 141, 2494-2505 doi:10.1242/dev.101790

RESEARCH ARTICLE

The facial neural crest controls fore- and midbrain patterning by regulating Foxg1 expression through Smad1 activity

Diego P. Aguiar*, Soufien Sghari and Sophie Creuzet‡

ABSTRACT

The facial neural crest (FNC), a pluripotent embryonic structure forming craniofacial structures, controls the activity of brain organisers and stimulates cerebrum growth. To understand how the FNC conveys its trophic effect, we have studied the role of *Smad1*, which encodes an intracellular transducer, to which multiple signalling pathways converge, in the regulation of *Foxg1*. *Foxg1* is a transcription factor essential for telencephalic specification, the mutation of which leads to microcephaly and mental retardation. *Smad1* silencing, based on RNA interference (RNAi), was performed in pre-migratory FNC cells. Soon after electroporation of RNAi molecules, *Smad1* inactivation abolished the expression of *Foxg1* in the chick telencephalon, resulting in dramatic microcephaly and partial holoprosencephaly. In addition, the depletion of *Foxg1* activity altered the expression *Otx2* and *Foxa2* in di/mesencephalic neuroepithelium. However, when mutated forms of *Smad1* mediating Fgf and Wnt signalling were transfected into FNC cells, these defects were overcome. We also show that, downstream of *Smad1* activity, Dkk1, a Wnt antagonist produced by the FNC, initiated the specification of the telencephalon by regulating *Foxg1* activity. Additionally, the activity of *Cerberus* in FNC-derived mesenchyme synergised with *Dkk1* to control *Foxg1* expression and maintain the balance between *Otx2* and *Foxa2*.

KEY WORDS: Neural crest, Telencephalic hemispheres, RNAi, Holoprosencephaly, Electroporation, Chick

INTRODUCTION

The telencephalon is the most evolutionarily recent part of the central nervous system (CNS), and represents a salient trait of the vertebrate phylum. The specification of the telencephalon primarily relies on the transcription factor Foxg1 (Tao and Lai, 1992; Xuan et al., 1995; Hanashima et al., 2004; Martynoga et al., 2005; Manuel et al., 2010), which is expressed in the prosencephalic neuroepithelium and is involved in segregating the telencephalon from the diencephalon. Investigations directed towards understanding forebrain regionalisation have demonstrated the importance of the anterior neural ridge (ANR) as the 'prosencephalic brain organiser', through the production of Fgf8 signal (Shimamura and Rubenstein, 1997; Houart et al., 1998; Shanmugalingam et al., 2000; Storm et al., 2006). Removal of ANR completely inhibits *Foxg1* expression and leads to the loss of telencephalic structures. Deficits can be overcome by supplying an exogenous source of Fgf8 (Shimamura and Rubenstein, 1997). Other brain-organising centres secreting Wnt and Shh molecules along the dorsal and ventral midlines are also required for brain development (McMahon and Bradley, 1990; Kim et al., 2001; Chang et al., 2004; Danesin et al., 2009; Vieira et al., 2010). Collectively, these factors generate a matrix of combinatorial morphogenetic factors, which governs planar specification and imparts a certain degree of molecular regionalisation to the cerebral neuroepithelium (Echevarría et al., 2003; Hoch et al., 2009).

Embryological studies have shown that the cephalic neural crest, which develops concomitantly to the formation of the CNS in vertebrates, is essential for brain development (Creuzet, 2009; Le Douarin et al., 2012). Neural crest cells originating from the posterior diencephalon down to rhombomere 2 (r2) provide the skeletogenic cells that build the facial structures and generate the musculo-connective cells lining the endothelium of blood vessels of the face and forebrain. This domain is here designated as FNC (facial neural crest). Absence of FNC prevents the formation of facial structures and also results in anencephaly: agenesis of telencephalic vesicles, thalamic and pre-tectal nuclei ensue (Creuzet et al., 2004, 2006). Brain defects occurring in the absence of the FNC stem from perturbations in the morphogenetic activities of secondary brain organisers: FNC ablation is promptly followed by loss of *Fgf8* in the ANR, loss of *Wnt* activity dorsally, and expansion of Shh ventrolaterally (Creuzet et al., 2006). It turns out that, during their migration, FNC cells shield and protect the brain against the detrimental effects of bone morphogenetic proteins (Bmps) secreted by neighbouring tissues, and promote Fgf8 activity in ANR (Creuzet, 2009). However, to a large extent, the repertoire of the FNC-produced molecules required for brain patterning remain unknown.

To explore this mechanism further, we have focused our interest on *Smad1*, which is expressed in pre-migratory FNC cells. Smad1 acts like a 'platform' upon which multiple signals converge: it is a transducer of the Bmp pathway and it mediates Fgf and Wnt signalling (Gont and Lough, 2000; Fuentealba et al., 2007). Here, we show that *Smad1* silencing in chick FNC cells inhibits *Foxg1* activity in the telencephalon and causes a severe microcephaly and partial holoprosencephaly. At the di/mesencephalic level, *Smad1* silencing reduces *Otx2* expression and triggers a concomitant expansion of *Foxa2* ventrolaterally, molecular changes that are attributable to the loss of *Foxg1* in the telencephalon. We have sought downstream effectors and identified two modulators of the Wnt pathway, Dkk1 and Cerberus. Analysis of their epistatic relationships shows that these molecules, produced by the migratory FNC cells, cooperate under the control of *Smad1* activity to control *Foxg1* expression in the telencephalon and regulate the balance between *Otx2* and *Foxa2* at the di/mesencephalic level.

RESULTS

Smad1 is expressed in pre-migratory FNC cells

Smad1 gene expression pattern was analysed by whole-mount *in situ* hybridisation in chick embryos from the neurula stage

Institut de Neurobiologie, Laboratoire de Neurobiologie et Développement, Avenue de la Terrasse, Gif-sur-Yvette 91198, France.
*Present address: Instituto de Ciências Biomédicas, Universidade Federal do Rio de Janeiro, Rio de Janeiro 21941-902, Brazil.

‡Author for correspondence (sophie.creuzet@inaf.cnrs-gif.fr)

Received 26 July 2013; Accepted 22 April 2014

Development (2014) 141, 2494-2505 doi:10.1242/dev.101790

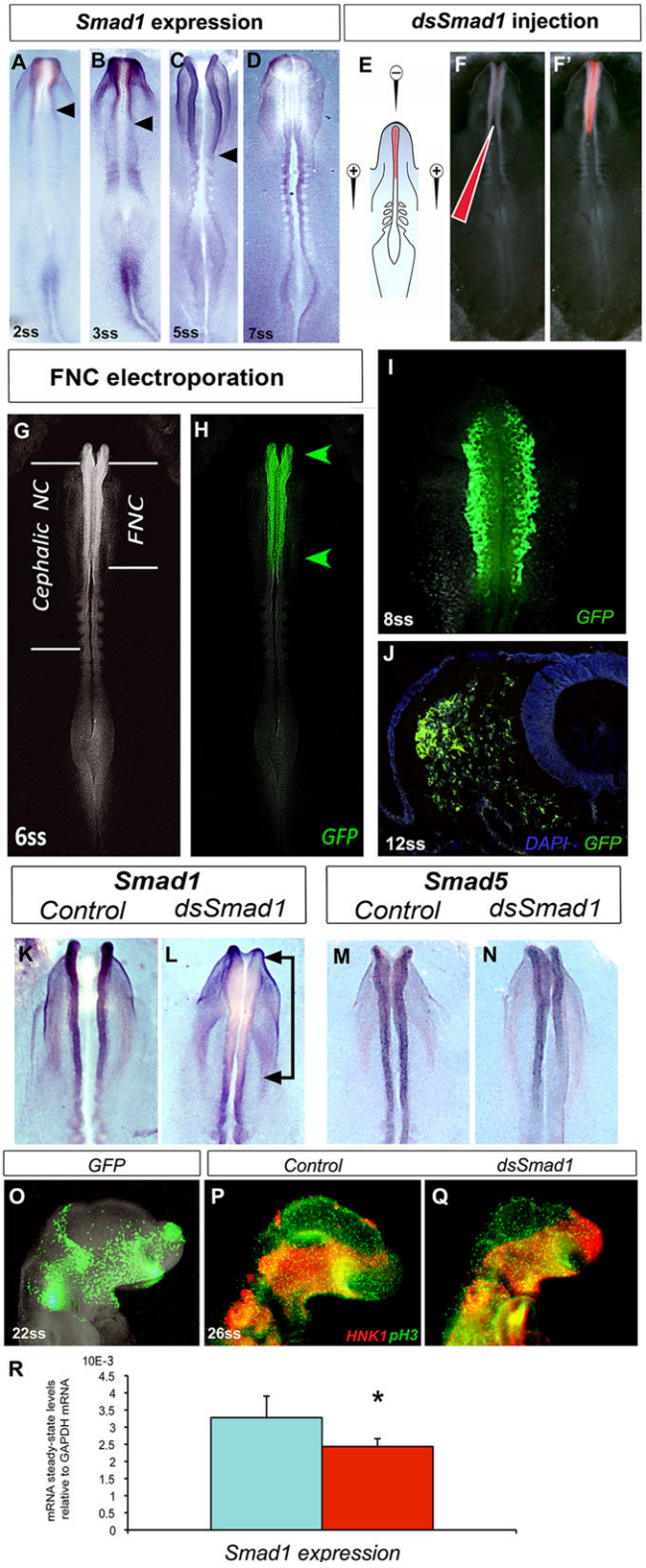

Fig. 1. Specificity of *Smad1* silencing in FNC cells. (A-D) *Smad1* expression at 2ss, 3ss, 5ss and 7ss. Arrowheads indicate the caudal limit of gene expression. (E-F′) Injection of *dsSmad1* plus Rhodamine Dextran (in red) and a pCAGGS-GFP construct in the neural tube at 4ss. (G,H) Whole-mount embryo at 6ss (G) and GFP labelling of FNC cells at 6ss after bilateral electroporation (H). NC, neural crest. Arrowheads indicate the limits of the transfected territory. (I) GFP-positive FNC cells migrate laterally at 8ss, and the telencephalon remains untransfected. (J) Tranverse section at the mesencephalic level showing GFP-positive FNC cells; the neuroepithelium and superficial ectoderm are devoid of any labelling. (K-N) *In situ* hybridisation for *Smad1* (K,L) and *Smad5* (M,N) at 5ss, 90 min after electroporation. Arrows in L indicate the FNC where Smad1 is silenced. (O-Q) Lateral views of 26ss embryos. (O) GFP-positive migrating cells in the maxillo-mandibular and nasofrontal buds. (P,Q) Immunolabelling with HNK1 (in red) and anti-pH3 (in green) antibodies in control (P) and *dsSmad1*-electroporated (Q) embryos. (R) Quantification of *Smad1* expression in control (blue) and *dsSmad1*-treated (red) embryos by qRT-PCR at 25ss (mean±s.e.m.; **P*<0.0125).

onwards. In early neurula (2-somite stage; ss), *Smad1* transcripts were detected at the margin of the neural plate in the presumptive diencephalon and mesencephalon, and, to a lesser extent, in cephalic superficial ectoderm (Fig. 1A). Before neural tube closure, *Smad1* expression gained in intensity in the neural fold (NF) and was extended down to the anterior rhombencephalic NF at 3ss (Fig. 1B), and further down to the level of r6 at 5ss (Fig. 1C). At 7ss, *Smad1* expression was rapidly switched off in FNC cells that had emigrated from the cephalic NF (Fig. 1D). Caudally, where the neural plate was still open, the accumulation of *Smad1* transcripts was intense. Later on, *Smad1* expression was observed in the FNC-derived mesenchymal cells that had colonised naso-frontal and maxillo-mandibular buds at 26ss.

Smad1 silencing in FNC cells results in morphological defects of brain development

To unravel the role of *Smad1* expression in FNC cell on brain development, double-stranded RNA molecules were designed against chick *Smad1* (*dsSmad1*), and bilaterally electroporated into the FNC cells at 4ss, when *Smad1* expression is maximal in the cephalic NF. FNC cells were specifically transfected, as attested by the co-electroporation of Rhodamine Dextran and a GFP construct (Fig. 1E-H). At 8ss, FNC cells have migrated laterally, but the telencephalic territory is devoid of GFP labelling (Fig. 1I). At 12ss, the transfected FNC cells that have emigrated from the neural plate border are GFP positive, but the roof plate and the alar plate of the brain are GFP negative (Fig. 1J). The efficacy of *Smad1* silencing was tested by whole-mount hybridisation (Fig. 1K-N). Ninety minutes after electroporation (i.e. 5ss), *Smad1* expression was abolished in FNC cells (Fig. 1K,L), but the expression of other Smad genes, such a *Smad5*, were unaffected (Fig. 1M,N). At 22ss, GFP-labelled FNC cells have colonised the naso-frontal and maxillo-mandibular buds (Fig. 1O). Co-immunostaining with HNK1 and anti-phosphorylated histone3 (pH3) antibodies to demonstrate FNC cell migration and cell proliferation, respectively, confirmed that *Smad1* silencing did not affect the capacities of FNC cells to populate the facial processes (Fig. 1P,Q). qRT-PCR assays were carried out with total RNAs extracted from pre-otic heads harvested 20 h after electroporation, to determine the steady-state levels of *Smad1* mRNAs (Fig. 1R). In the *dsSmad1*-treated series, *Smad1* transcript accumulation shrank to 30% relative to controls.

The morphological changes after *Smad1* silencing were observed at 26ss. Compared with controls, we noted that repression of *Smad1* activity in FNC cells caused severe fore- and midbrain malformations (n=76; Fig. 2A,B). Cephalic vesicles were atrophied and the subdivision of prosencephalon into tel- and diencephalon was no longer visible (Fig. 2B, arrowheads). At embryonic day (E) 4 (n=14), head morphogenesis in experimental embryos was affected by severe telencephalic atrophy: the development of the nasofrontal and mandibular processes was reduced. Notably, the telencephalic territory displayed a partial holoprosencephaly (Fig. 2C,D, asterisk). To characterise brain defects further, morphometric analysis was performed by measuring the impact of *Smad1* silencing on the growth

Development (2014) 141, 2494-2505 doi:10.1242/dev.101790

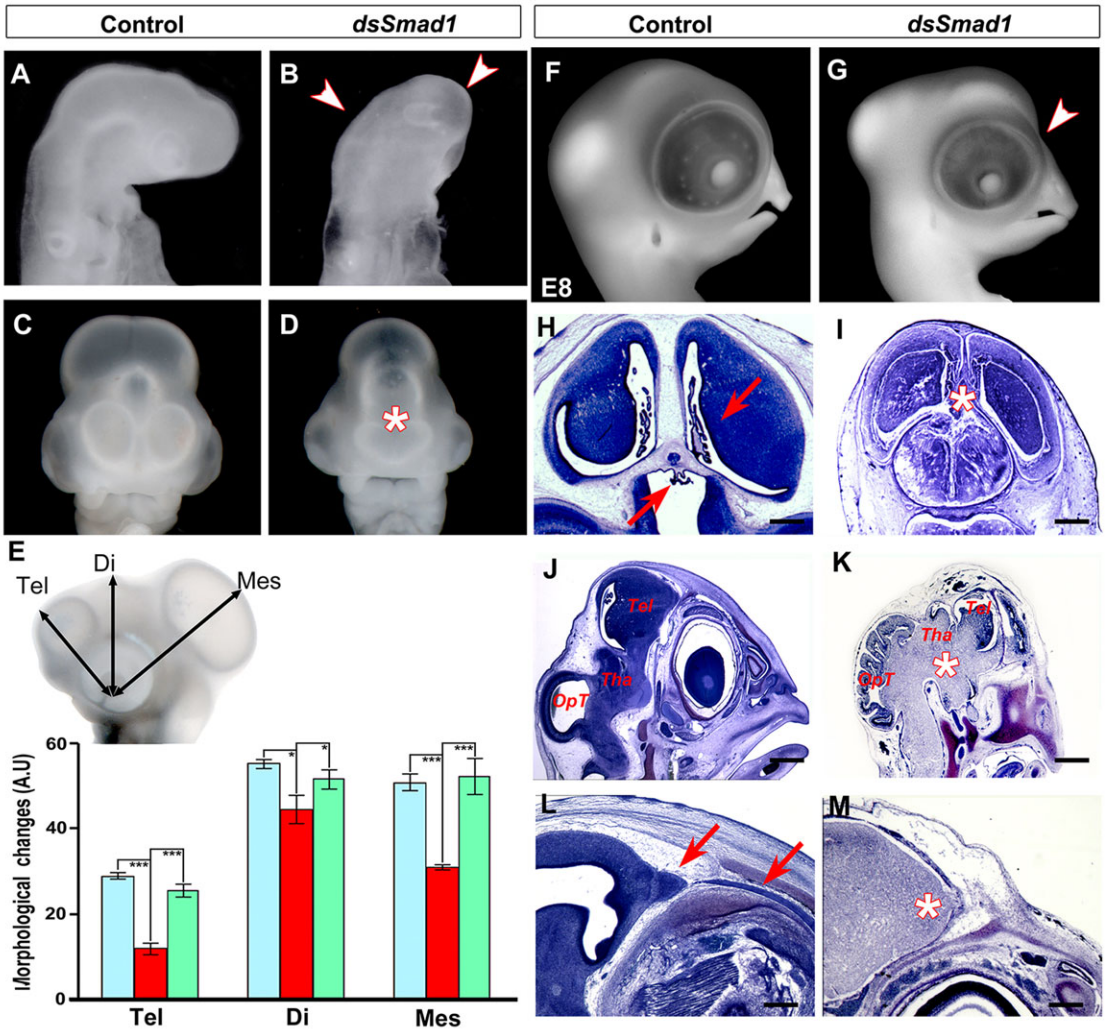

Fig. 2. *Smad1* silencing in FNC cells results in brain malformations. (A-D) Morphology of control and *dsSmad1*-electroporated embryos at 24ss (A,B; lateral view) and E4 (C,D; fontal view). Arrowheads and asterisk indicate the cephalic atrophy. (E) Morphometric analysis of brain development: distance between the lens and the dorsal telencephalon (Tel), the epiphysis (Di) and the optic tectum (Mes) in control (blue), *dsSmad1*-transfected (red) and *dsSmad1*/*hSmad1* co-electroporated (green) embryos (mean±s.e.m.; **P*<0.0125, ****P*<0.0001). (F,G) Morphology of control and *dsSmad1*-transfected embryos at E8 showing fronto-nasal defects on lateral view (G; arrowhead). (H,I) Coronal sections of control (H) and *dsSmad1*-electroporated (I) embryos. Note that the choroid plexuses (arrows in H) are reduced (asterisk in I) and the ventricles collapsed after *Smad1* silencing. (J-M) Para-sagittal sections of E8 control (J,L) and *dsSmad1*-transfected (K,M) embryos showing ventral expansion of the brain (K, asterisk). On mesial sections, the olfactory bulbs and nerves, present in control (L; arrows), are missing in *dsSmad1*-transfected embryos (M; asterisk). OpT, optic tectum; Tel, telencephalon; Tha, thalamus. Scale bars: 1 mm (J-O); 300 µm (H,I).

of tel-, di- and mesencephalic vesicles (Fig. 2E). The microcephalic phenotype was particularly pronounced anteriorly, where the telencephalic hemispheres only represented 40% of the normal size (Fig. 2C). In addition, the optic vesicles were also hypoplastic in *dsSmad1*-electroporated embryos.

Induction of long-term defects in cephalic development by *Smad1* loss of function in FNC cells at E8 (Fig. 2F,G) were examined through structural staining of coronal sections (Fig. 2H,I). Telencephalic hemispheres exhibited severe disorganisation: the lateral and third ventricles were collapsed and the choroid plexi were hypoplastic (Fig. 2H,I), and the septal region was atrophied (Fig. 2I, asterisk). Para-sagittal sections revealed that the ventrolateral part of the pre-otic brain, from the thalamus down to the level of the anterior rhombencephalon was considerably expanded in *dsSmad1*-treated embryos compared with controls (Fig. 2J,K, asterisk). In addition, on mesial sections, in the olfactory bulbs, the olfactory nerves (Fig. 2L, arrows) were missing (Fig. 2M, asterisk). Altogether, these observations showed that repressing *Smad1* activity in FNC cells had adverse effects on brain development.

To show that the morphological defects were specifically due to *Smad1* inactivation, we tried to rescue cephalic development by co-electroporating *dsSmad1* with a construct driving the expression of a wild-type form of human *SMAD1* (*hSmad1*). We first tested the innocuity of the *hSmad1* construct on cephalic development by transfecting this plasmid alone. We observed that *hSmad1* did not cause any alteration of head morphogenesis at 26ss (*dsSmad1*/*hSmad1*; *n*=22). In a next step, *hSmad1* construct was co-electroporated with *dsSmad1* in the FNC at 4ss (*n*=42). Twenty-four hours post-transfection, *dsSmad1*/*hSmad1* embryos showed a significant rescue of their cephalic development compared with *dsSmad1*-electroporated embryos (Fig. 3). Hence, the heterospecific restoration of *Smad1* activity was sufficient to overcome defects resulting from *Smad1* silencing.

Development (2014) 141, 2494-2505 doi:10.1242/dev.101790

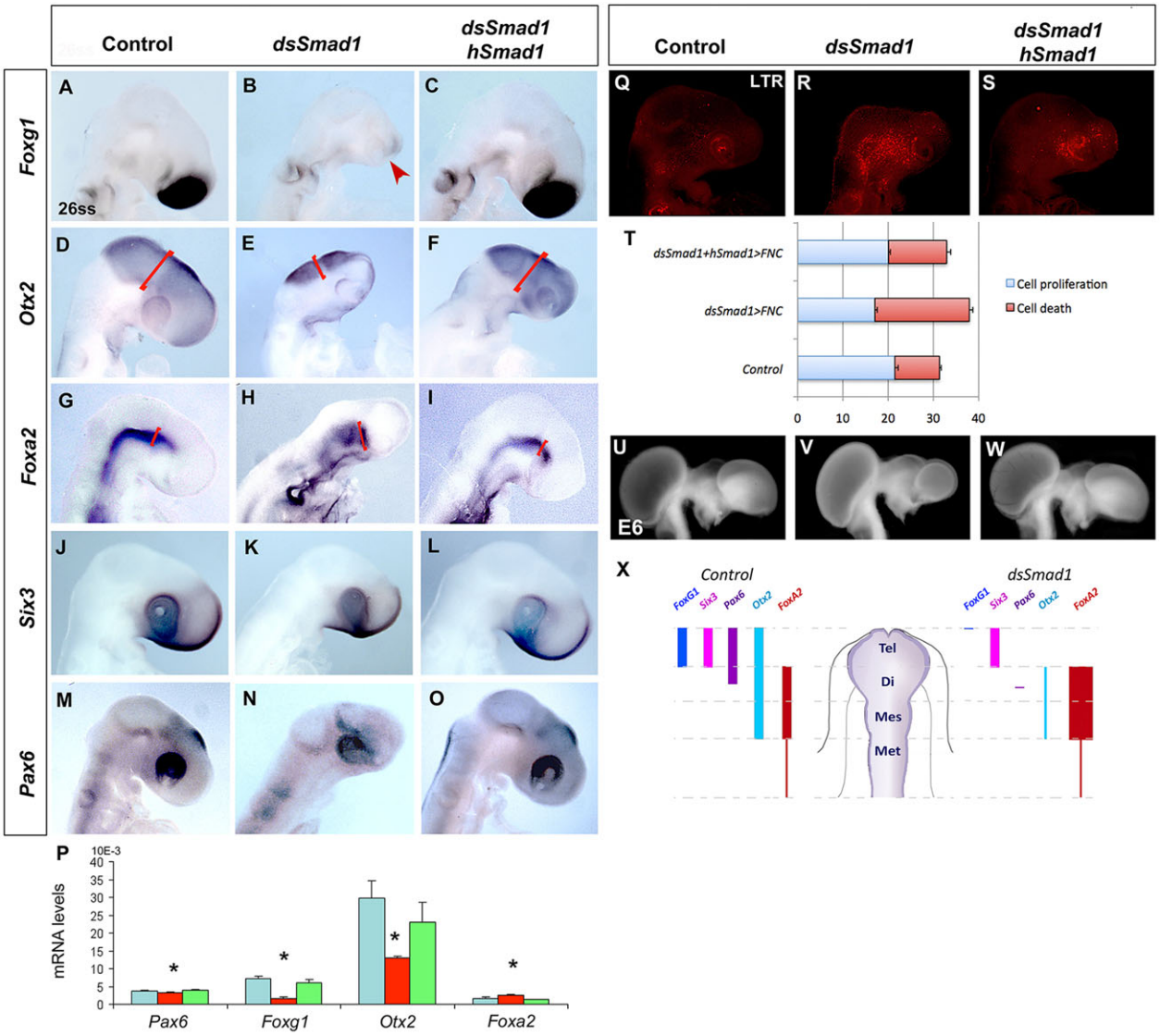

Fig. 3. *Smad1* silencing alters brain patterning. (A-O) Lateral views of 26ss control (A,D,G,J,M), *dsSmad1*-transfected (B,E,H,K,N) and *dsSmad1*/*hSmad1*-transfected (C,F,I,L,O) embryos. Hybridisation for *Foxg1* (A-C), *Otx2* (D-F), *Foxa2* (G-I), *Six3* (J-L) and *Pax6* (M-O). Red brackets in D-I point to changes in *Otx2* and *Foxa2* expression. Arrowhead in B indicates the loss of *Foxg1* expression in the telencephalon. (P) Quantification of *Pax6*, *Foxg1*, *Otx2* and *Foxa2* expression by qRT-PCR in control (blue) and *dsSmad1*-silenced (red) embryos. These changes tend to normalise when *dsSmad1* molecules are co-electroporated with *hSmad1* constructs (green) (mean±s.e.m.; *P<0.0125). (Q-S) LTR staining of control (Q), *dsSmad1*-treated (R) and *dsSmad1+hSmad1*-transfected (S) embryos. *Smad1* silencing in the FNC augments cell death in the developing head. (T) Quantification of cell proliferation (blue) and cell death (red) in control and experimental series (mean±s.e.m.). (U-W) Side views showing brain morphology of E6 control (U), *dsSmad1*-transfected (V) and *dsSmad1*/*hSmad1* co-electroporated (W) embryos. (X) Diagram recapitulating molecular changes in brain patterning after *Smad1* silencing. Coloured bars represent expression domains of the listed genes. Di, diencephalon; Mes, mesencephalon; Met, metencephalon; Tel, telencephalon.

Smad1 silencing in FNC cells entails molecular changes in brain development

In our experiments, perturbations of brain development in *dsSmad1*-depleted embryos were first observed at 26ss. To elucidate the molecular mechanisms involved in cephalic hypoplasia, expression of transcription factors involved in brain patterning were analysed at 26ss. *Foxg1*, which is the earliest marker of telencephalic vesicles (Xuan et al., 1995; Chapman et al., 2002), was strongly expressed in control embryos (Fig. 3A). Knocking down *Smad1* abrogated its expression (Fig. 3B, red arrowhead; n=30), but the co-electroporation of a *dsSmad1* and *hSmad1* construct normalised *Foxg1* activity and forebrain development (Fig. 3C; n=25).

Otx2 expression, which characterises the anterior neural plate at neurula stage (Acampora et al., 1998; Plouhinec et al., 2005), is detected in the telencephalon, and in the alar plate of the di- and mesencephalon at 26ss (Fig. 3D). In absence of *Smad1* in FNC cells, *Otx2* domain expression was reduced and limited at the dorsal midline of the di- and mesencephalon (Fig. 3E; n=20). Strikingly, *Otx2* expression was completely lost in the telencephalic vesicles of *Smad1*-silenced embryos. Electroporation of the *hSmad1* construct tended to normalise *Otx2* activity in the fore- and midbrain (Fig. 3F; n=15). We also looked at the expression of *Foxa2*, a marker of di- and mesencephalic basal plate (Ruiz i Altaba et al., 1995) (Fig. 3G). In *dsSmad1*-electroporated embryos, *Foxa2* expression was considerably expanded dorsally (Fig. 3H; n=18), and also upregulated in foregut endoderm. When *Smad1* activity was restored by the co-electroporation of *hSmad1*, its expression was restricted to the basal plate (Fig. 3I; n=16). *Six3* is strongly

Development (2014) 141, 2494-2505 doi:10.1242/dev.101790

expressed along the anteroventral midline of the telencephalon in normal embryos (Geng et al., 2008). *Six3* expression was not significantly perturbed by the loss of function of *Smad1* in FNC cells (in comparison with the absence of *Foxg1* activity) or by the co-electroporation of *hSmad1* (Fig. 3J-L). We also looked at the expression of *Pax6*, as a marker of the retinal primordium (Walther and Gruss, 1991), transcripts of which are accumulated in the optical vesicles and in the epithalamus (Fig. 3M). In the absence of *Smad1*, the hypoplasia of developing eyes coincided with severe reduction of *Pax6* (Fig. 3N; *n*=12), but this default was rescued by co-electroporating *hSmad1* (Fig. 3O; *n*=10). Molecular changes occurring in cephalic vesicles after *Smad1* silencing in FNC cells were quantified by qRT-PCR performed on developing heads 20 h post-electroporation (Fig. 3P). The quantification of gene expression revealed that *dsSmad1* altered the activity of *Pax6* (*Pax6*Δ=11%), *Foxg1* (*Foxg1*Δ=75%) and *Otx2* (*Otx2*Δ=55%). By contrast, in *Smad1*-silenced embryos, *Foxa2* expression was significantly increased up to 1.5-fold compared with controls. As expected from whole-mount hybridisations, in embryos co-electroporated with a *dsSmad1* and *hSmad1* construct, gene expression was restored to the levels detected in controls. To see if cellular events could account for the molecular changes, whole-mount detection of cell death was performed. In controls, punctate Lysotracker Red (LTR) labelling was scarcely observed in the retroocular region, where FNC cells migrate (Fig. 3Q). In *dsSmad1*-treated embryos, LTR staining was considerably expanded (Fig. 3R), but electroporation with *hSmad1* alleviated cell death (Fig. 3S). Whatever the series, the dorsal aspects of the fore-and midbrain remained unaffected. Quantifications on sections further documented the impact of *Smad1* silencing on cell proliferation and death, and the restoration after *hSmad1* electroporation (Fig. 3T). Normalisation of cellular events in embryos and the molecular profile of the developing brains at 26ss after the co-electroporation of *dsSmad1* and *hSmad1* ended up with a significant restoration of prosencephalic development at E6 (Fig. 3U-W).

Here, we show that silencing *Smad1* activity in FNC cells is sufficient to turn off *Foxg1* activity. More caudally, in the di- and mesencephalon, *Smad1* inactivation also resulted in a dramatic reduction of *Otx2* and the expansion of *Foxa2* (Fig. 3X). The mutual opposition of these two genes has been previously documented and accounted for by a balance between 'dorsalising' versus 'ventralising' processes of the pre-otic neuroepithelium (Nakano et al., 2000; Ang et al., 1996). In our experiments, the misregulation of *Smad1* in FNC cells turns out to favour *Foxa2* expansion and *Otx2* reduction: this condition ends up with a potent ventralisation of the di- and mesencephalic territory.

Changes in signalling triggered by *Smad1* silencing

Perturbations in the expression of transcription factors suggested that crucial changes in the morphogenetic activity of 'secondary brain organisers' had occurred in absence of *Smad1* activity in FNC cells. Production of *Fgf8* in the ANR has been shown to play a leading role in telencephalic patterning (Shimamura and Rubenstein, 1997; Houart et al., 1998; Shanmugalingam et al., 2000). In controls, *Fgf8* domain of expression is maximal at 26ss. In *dsSmad1*-electroporated embryos, a weak reduction of its domain was observed (Fig. 4A-C; *n*=15). *Bmp4* expression, normally present in the superficial naso-frontal ectoderm surrounding the ANR (Fig. 4D), was upregulated in the retroocular (i.e. presumptive maxillary) region after *dsSmad1* silencing (Fig. 4E,F: *n*=10). In the basal plate, *Shh* is the major signal to be produced and has a deep

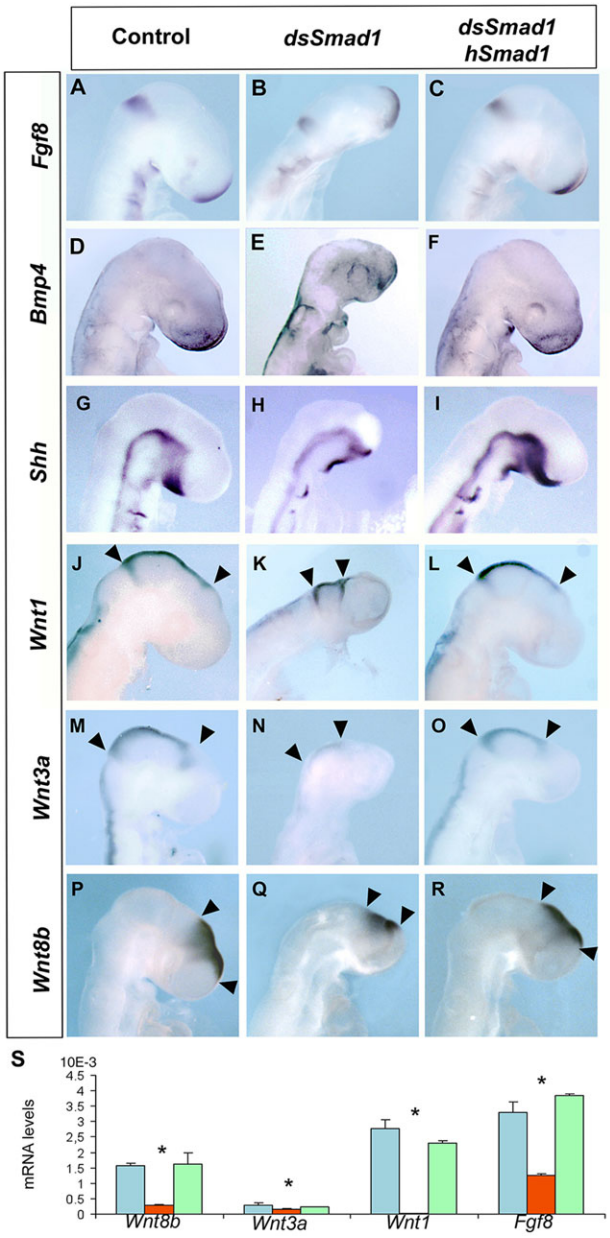

Fig. 4. Modulation of morphogen activity after *Smad1* silencing. (A-R) Lateral views of hybridisations in control, *dsSmad1*- and *dsSmad1*/*hSmad1*-transfected embryos for *Fgf8* (A-C), *Bmp4* (D-F), *Shh* (G-I), *Wnt1* (J-L), *Wnt3a* (M-O) and *Wnt8b* (P-R). Arrowheads indicate the domain of expression. (S) Quantification of *Wnt8b*, *Wnt3a*, *Wnt1* and *Fgf8* expression in control (blue), *dsSmad1*-treated (red) and *dsSmad1*+*hSmad1*-transfected (green) embryos determined by qRT-PCR (mean±s.e.m.; **P*<0.0125).

impact on brain patterning (Vieira and Martinez, 2006). In *dsSmad1*-treated embryos, *Shh* expression was not reduced, but was maintained in proportion with the global prosencephalic hypoplasia (Fig. 4G-I; *n*=12).

At the dorsal midline, Wnt signalling is essential for fore- and midbrain patterning (Erter et al., 2001; Braun et al., 2003; Creuzet et al., 2004). *Wnt1*, which is expressed at the dorsal midline and by a strand of cells adjacent to the isthmus, was reduced dorsally in *dsSmad1*-electroporated embryos (Fig. 4J-L, arrowheads). *Wnt3a*, which has an overlapping domain of expression with *Wnt1* at the midline, was absent in *dsSmad1*-electroporated embryos (Fig. 4M-O, arrowheads; *n*=13). *Wnt8b*, expression of which dorsally straddles

Development (2014) 141, 2494-2505 doi:10.1242/dev.101790

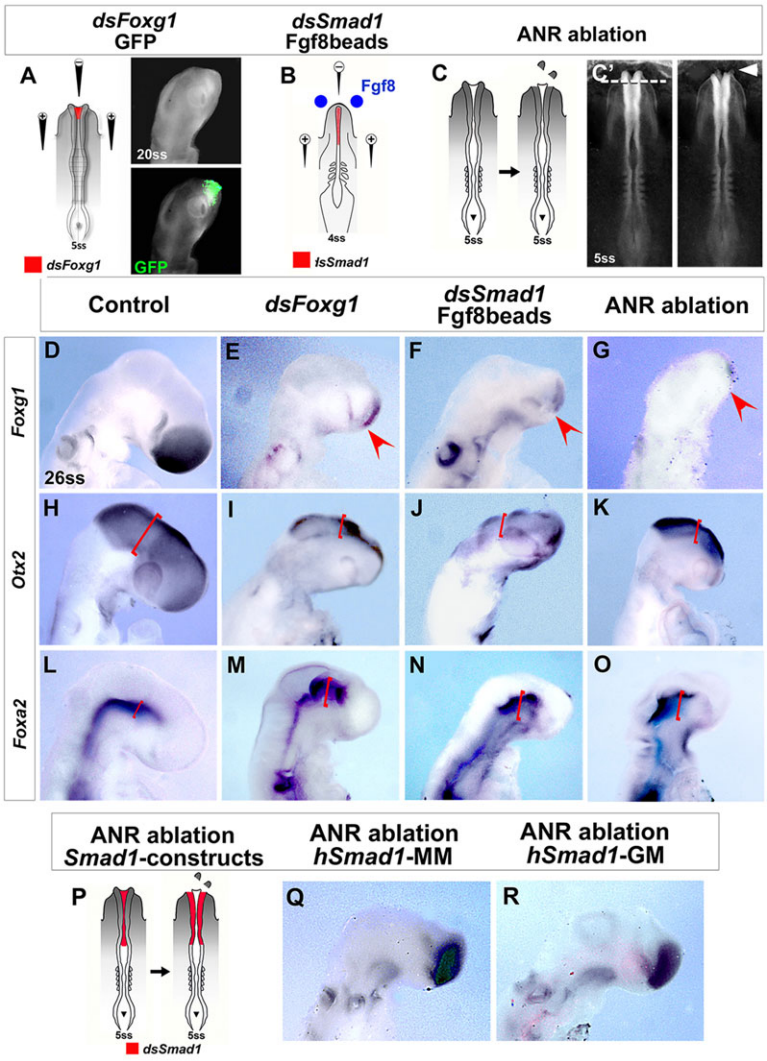

Fig. 5. Control of *Foxg1* expression by *Smad1* activity in the FNC. (A) Bilateral electroporation of *dsFoxg1* in the telencephalon at 5ss (left). GFP labelling of electroporated site on lateral view at 20ss (right). (B) *dsSmad1* bilateral electroporation in the FNC (red) and Fgf8-soaked beads implantation in the ANR (blue). (C,C′) ANR ablation (dashed line; arrowhead) at 5ss. (D-O) Hybridisation at 26ss for *Foxg1* (D-G), *Otx2* (H-K) and *Foxa2* (L-O) in control (D,H,L), *dsFoxg1*-transfected (E,I,M), *dsSmad1*-transfected+Fgf8-supplemented (F,J,N) and ANR-ablated embryos (G,K,O). (P) ANR ablation and FNC electroporation with constructs driving mutated forms of *Smad1* at 5ss (red). (Q,R) Hybridisation for *Foxg1* in *hSmad1*-MM- (Q) and *hSmad1*-GM- (R) transfected embryos at 26ss.

the anterior diencephalon and posterior telencephalon, was decreased in both vesicles after *Smad1* silencing (Fig. 4P-R; n=12). Changes in gene expression were quantified by qRT-PCR (Fig. 4S): *Smad1* silencing significantly affected the activity *Fgf8* (*Fgf8*Δ=60%), *Wnt1* (*Wnt1*Δ=40%), *Wnt3a* (*Wnt3a*Δ=80%) and *Wnt8b* (*Wnt8b*Δ=30%). Therefore, these results indicated that *Smad1* silencing primarily affected Fgf and Wnt production in the developing brain.

Foxg1 loss of function reproduces *Smad1* silencing in the FNC

To explore whether the loss of *Foxg1*, on its own, can have an effect on the expression of *Otx2* and *Foxa2*, *Foxg1* expression was silenced in the telencephalon, specifically, leaving FNC cells unperturbed. dsRNA designed against *Foxg1* (*dsFoxg1*) was bilaterally electroporated at 5ss (Fig. 5A). At 26ss, *Foxg1* activity was abrogated in the prosencephalon (Fig. 5D,E; n=18); additionally, *Otx2* expression was limited to the roof-plate (Fig. 5H,I, red brackets; n=12) and *Foxa2* expression expanded in the lateral aspects of the di- and mesencephalon (Fig. 5L,M, red brackets; n=13). So, *Foxg1* silencing in telencephalon interfered with the patterning of more caudal structures, the thalamus and the optic tectum through the regulation of *Otx2* and *Foxa2*. This condition virtually recapitulated the molecular changes resulting from *Smad1* inactivation in FNC cells (compare with Fig. 3). These observations indicated that, in normal development, the regulation of *Foxg1* activity is central to the molecular patterning of the pre-otic brain.

Dissecting the interactions involved in Foxg1 expression

Current understanding of prosencephalon development suggests a direct relationship between *Fgf8* activity from the ANR and the induction of *Foxg1* expression in the ANR and its expansion to the entire telencephalon (Shimamura and Rubenstein, 1997; Houart et al., 1998; Hoch et al., 2009; Anderson et al., 2002). Therefore, we tested if supplying *Fgf8* could bypass the effect of *Smad1* silencing and rescue *Foxg1* expression in *dsSmad1*-electroporated embryos. Beads soaked with Fgf8 recombinant protein (0.125 µg/µl) were implanted in contact with the ANR in a 4ss embryo subjected to *Smad1* silencing (Fig. 5B). This concentration has been previously shown to restore cephalic development efficiently when endogenous expression of Fgf8 in ANR was abolished after FNC ablation (Creuzet et al., 2006). Here, despite Fgf8 supplementation, no restoration of telencephalic development occurred and *Foxg1* expression was absent, as in *Smad1*-silenced embryos (Fig. 5D,F; n=9). In addition, the domain of *Otx2* expression exhibited no restoration and remained similar to that in *dsSmad1*-electroporated embryos, and *Foxa2* expression did not

Development (2014) 141, 2494-2505 doi:10.1242/dev.101790

tend to normalise (Fig. 5H,J,L,N; *n*=9). Altogether, our results indicated that *Foxg1* activity in the telencephalon does not solely depend on the production of Fgf8 in ANR, but relies on a more complex mechanism, which involves FNC cells, for its induction and expansion.

Stimulating *Smad1* activity in FNC cells can rescue *Foxg1* expression in the telencephalon

To decipher the mechanisms responsible for *Foxg1* expression in the telencephalon, we performed surgical ablation of the ANR at 5ss, before FNC cell migration (Fig. 5C,C′). At 26ss, the morphology of the telencephalon was atrophied, and *Foxg1* expression was abolished in ANR-ablated embryos (Fig. 5G), as previously reported (Shimamura and Rubenstein, 1997). Additionally, *Otx2* and *Foxa2* expressions were perturbed and displayed a pattern similar to that observed in *dsSmad1*- and *dsFoxg1*-electroporated embryos (Fig. 5I,K,M,O; compare with Fig. 3E,H).

To examine if FNC cells could regulate *Foxg1* expression in the telencephalon independently of the production of *Fgf8* in the ANR, we transfected mutated forms of *hSmad1* in FNC cells to rescue the molecular patterning of the pre-otic brain in ANR-ablated embryos (Fig. 5P). These constructs have been previously designed to mimic constitutive activation in the linker region for the Mapk (*hSmad1*-MM) and Gsk3 (*hSmad1*-GM) pathways, respectively (Fuentealba et al., 2007). When electroporated in FNC cells of ANR-ablated embryos, these constructs generated a potent restoration of *Foxg1* activity in the telencephalon (Fig. 5Q,R). Hence, the regulation of *Smad1* activity by the Fgf and Wnt pathways in FNC cells is essential to establish the domain of *Foxg1* expression in the developing prosencephalon.

Smad1 regulates the activity of Bmp antagonists in FNC cells

Previously, we have demonstrated that FNC cells play a crucial role in brain development by counteracting Bmp activity through the production of Bmp inhibitors (Creuzet, 2009). *Noggin*, a potent antagonist of Bmps is expressed in FNC cells before their migration and in FNC-derived mesenchyme of the naso-frontal and the retroocular region (Tzahor et al., 2003). In *Smad1*-silenced embryos, a strong reduction of *Noggin* activity was shown by RT-PCR at 26ss (Fig. 6A,B). This change was correlated with the loss of *Foxg1* and the misexpression of *Otx2* and *Foxa2* (Fig. 6B). RT-PCR and whole-mount hybridisation also revealed that *Smad1* silencing affected *Noggin* activity: its expression was downregulated as early as 5ss (2 h after *dsSmad1* electroporation; Fig. 6C,D). In the same way, *Gremlin*, another potent Bmp inhibitor (Merino et al., 1999), was also downregulated after *Smad1* silencing (Fig. 6E,F). Altogether, these observations showed that *Smad1* expression in FNC was crucial for the regulation of Bmp inhibitors from neurula stage up to 26ss.

To test the possible role of Bmp signalling in regulating *Foxg1* expression, the activity of *Noggin* and *Gremlin* was simultaneously silenced (*dsNoggin*/*dsGremlin*) in the FNC at 4ss. The joint inactivation of *Noggin* and *Gremlin* resulted in loss of *Foxg1* expression, together with misexpression of *Otx2* and *Foxa2* (Fig. 6G-N; *n*=9). These experiments indicated that loss of *Noggin* and *Gremlin* expression in FNC cells are involved in the molecular changes consecutive to *Smad1* silencing, therefore showing that *Smad1* expression controls the expression of Bmp antagonists produced by migratory FNC cells.

We then tried to rescue *Smad1* silencing with the joint electroporation of retroviral RCAS constructs driving *Gremlin* and *Noggin* expression (Fig. 6O). As a consequence, the cephalic

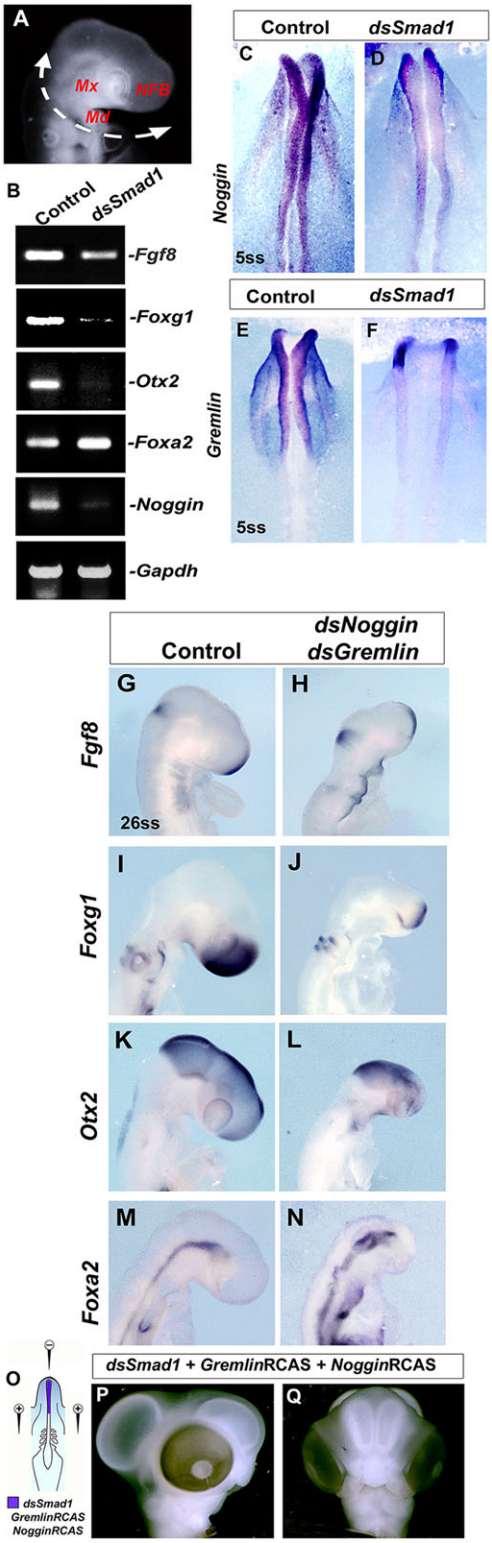

Fig. 6. *Smad1* expression controls *Noggin* and *Gremlin* activity. (A,B) Pre-otic head taken from a 26ss embryo (A) and subjected to RT-PCR analysis (B). (C-F) Hybridisation for *Noggin* (C,D) and *Gremlin* (E,F) in control and *dsSmad1*-silenced embryos. (G-N) Side views showing hybridisations for *Fgf8* (G,H), *Foxg1* (I,J), *Otx2* (K,L) and *Foxa2* (M,N) in controls and *Noggin*- and *Gremlin*-silenced embryos. (O-Q) Co-electroporation (O) of *dsSmad1*-, *Gremlin*+*Noggin*-RCAS. (P,Q) Profile (P) and frontal (Q) views showing rescued phenotype: *Gremlin*-*Noggin* expression bypass *Smad1* silencing to restore development of telencephalic hemispheres at E5. NFB, fronto-nasal bud; Md, mandibular process; Mx, maxillary process.

Development (2014) 141, 2494-2505 doi:10.1242/dev.101790

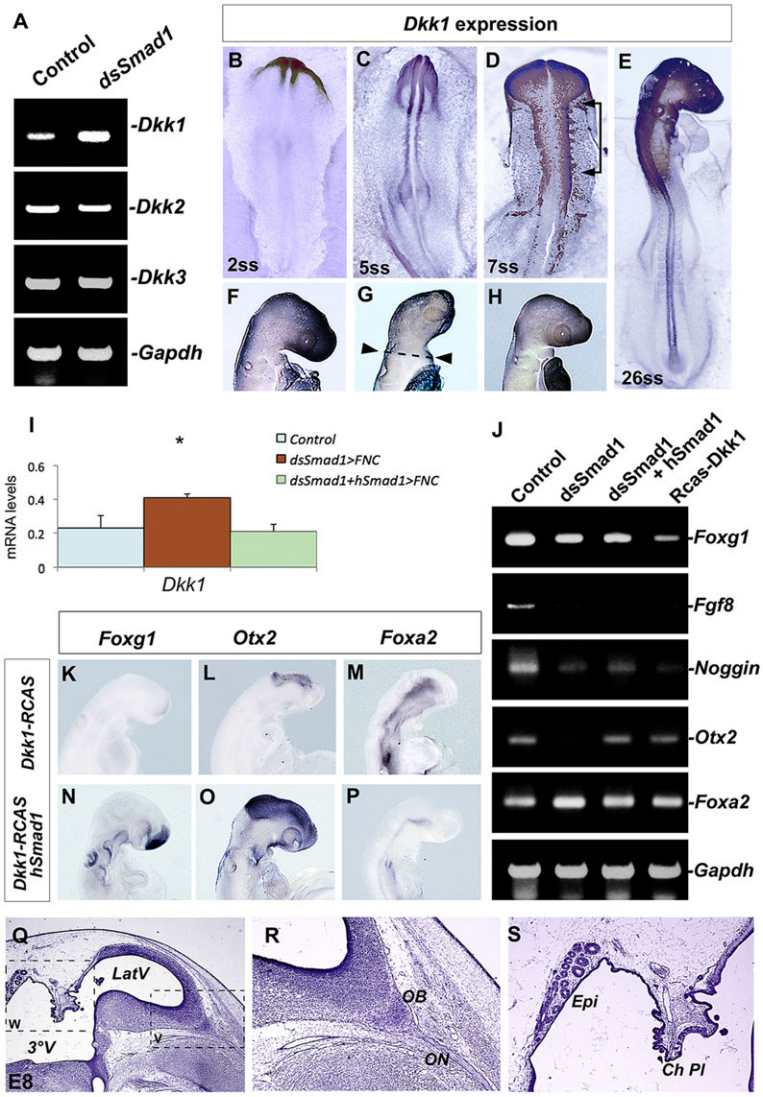

Fig. 7. Control of *Dkk1* expression by *Smad1* is essential for telencephalic development. (A) RT-PCR analysis of *Dkk1*, *Dkk2*, *Dkk3* gene expression in control and *dsSmad1*-treated embryos. (B-E) *Dkk1* is expressed in the head process at 2ss (B) and in the FNC and surface ectoderm at 5ss (C). *Dkk1* is expressed in migratory FNC cells at 7ss (D; arrow) and in FNC-derived mesenchyme at 26ss (E). (F-H) Lateral view showing hybridisation for *Dkk1* in control (F), *dsSmad1*-transfected (G) and *dsSmad1*/*hSmad1*-transfected (H) embryos. Dashed line in G delineates the distinct levels of *Dkk1* expression in pre-otic versus post-otic territories. (I) Quantification of *Dkk1* expression in control (blue), *dsSmad1*-treated (red) and *dsSmad1*+*hSmad1*-treated (green) embryos (mean±s.e.m.; **P*<0.0125). (J) RT-PCR showing expression of *Foxg1*, *Fgf8*, *Noggin*, *Otx2* and *Foxa2* in control and *dsSmad1*-, *dsSmad1*+*hSmad1*-, *Dkk1*-RCAS-transfected embryos. *Gapdh* is used as a normalizing gene. (K-P) Side view of hybridisation for *Foxg1* (K,N), *Otx2* (L,O) and *Foxa2* (M,P) in *Dkk1-RCAS*-electroporated (K-M) and *Dkk1-RCAS*/*hSmad1*-co-electroporated (N-P) embryos. (Q-S) Para-sagittal sections of *Dkk1-RCAS*/*hSmad1*-co-electroporated embryos showing rescued brain at E8. (R) The olfactory bulb (OB) and nerve (ON) have developed. (S) Along the diencephalic roof plate, choroid plexi (Ch Pl) and epiphysis (Epi) have formed. LatV, lateral ventricle; 3°V, third ventricle.

development tended to normalise: the telencephalon was no longer a holoprosencephalic vesicle, but developed as two hemispheres (Fig. 6P,Q; *n*=8). The rescued phenotypes showed that restoration of *Gremlin* and *Noggin* expression could bypass the defects of *Smad1* silencing. Altogether, these experiments bring compelling evidence that *Gremlin* and *Noggin* can together restore normal head and brain development, and act downstream of *Smad1* in FNC cells in this process.

Dkk1 expression in the FNC is subjected to *Smad1* activity

Another consequence of *Smad1* silencing was the upregulation of *Dkk1* expression in the FNC cell population at 26ss, while the level of *Dkk2* and *Dkk3* remained unchanged (Fig. 7A). *Dkk1*, a potent Wnt inhibitor, is required for the development of the anterior cephalic structures (Mukhopadhyay et al., 2001). In chick, *Dkk1* transcripts were detected in the NF and emigrating FNC cells (Fig. 7B-E), then became evenly distributed in the FNC-derived mesenchyme populating facial processes, thus leading to homogeneous staining of the developing head at 26ss (Fig. 7F). In *Smad1*-silenced embryos, increased activity of *Dkk1* was also demonstrated by *in situ* hybridisation: embryos exhibited a sharp difference in the level of *Dkk1* expression between the pre-otic head and the more caudal branchial arches, which were left unperturbed after *Smad1* silencing (Fig. 7G, dashed line; *n*=7). The upregulation of *Dkk1* was further confirmed by qRT-PCR analysis at 26ss (*Dkk1*Δ=1.8-fold higher than in control; Fig. 7I).

To understand the functional significance of *Dkk1* upregulation for brain patterning, a construct driving *Dkk1* expression (*Dkk1*-RCAS) was transfected into FNC cells at 5ss. Under this condition, the upregulation of *Dkk1* induced the same alterations in *Foxg1*, *Otx2* and *Foxa2* expression (Fig. 6 and Fig. 7J-M; *n*=9,7,8, respectively) as those triggered by *Smad1* silencing, thus indicating that changes in *Dkk1* activity in *dsSmad1* embryos accounted for the defects in brain patterning.

To explore the epistatic relationship between *Smad1* and *Dkk1* activity, we tried to restore brain patterning by forcing the expression of *hSmad1* in combination with *Dkk1*-RCAS in FNC cells at 5ss. When analysed at 26ss, embryos showed a significant rescue of *Foxg1*, *Otx2* and *Foxa2* expression (Fig. 7N-P). Restoration of the development of anterior and dorsal structures at the tel- and diencephalic level occurred at E8 (Fig. 7Q-S; compare with Fig. 2J,L). Therefore, we show that *Dkk1* expression in the FNC-derived mesenchyme is regulated by *Smad1* activity. These results also indicated that the adverse effects of *Smad1* silencing on brain development were due to the increased expression of *Dkk1* in FNC cells.

Development (2014) 141, 2494-2505 doi:10.1242/dev.101790

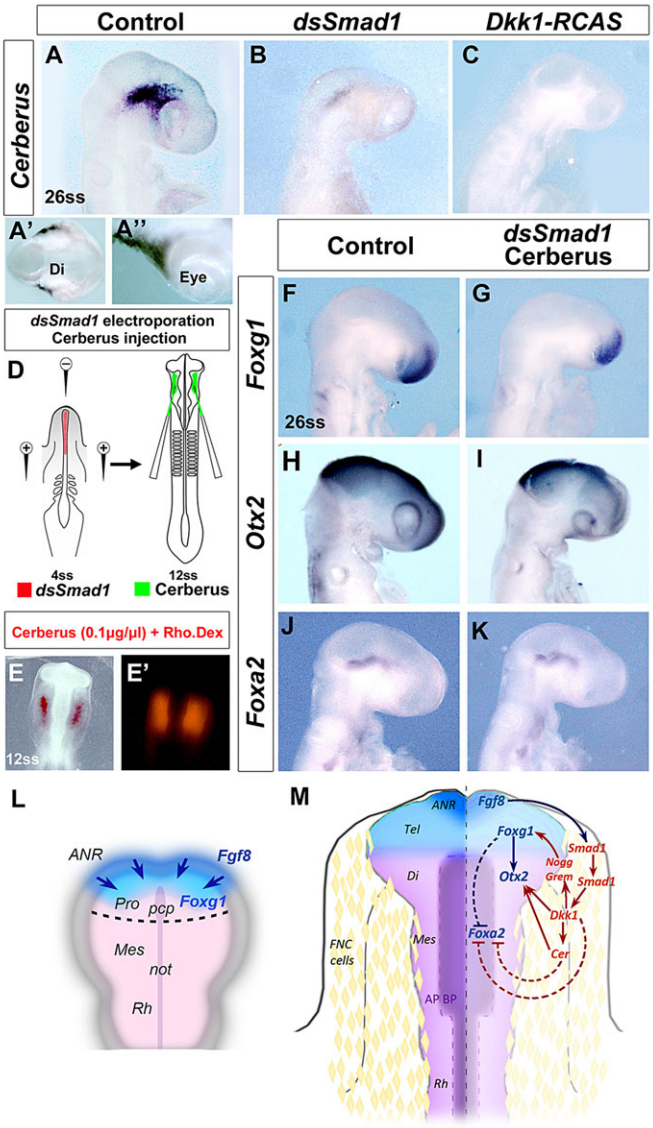

Fig. 8. Cerberus supplementation overcomes brain defects of *Smad1* silencing. (A-C) Side view of hybridisation for *Cerberus* in control, *dsSmad1*- and *Dkk1*-RCAS-transfected embryos at 26ss. (A′,A″) Vibratome section showing *Cerberus* expression in peri-ocular mesenchyme at 26ss. (D) *Smad1* silencing in the FNC at 4ss followed by bilateral injection of Cerberus protein into FNC-derived mesenchyme at 12ss. (E,E′) Cerberus protein contrasted with Rhodamine Dextran. (F-K) Hybridisation for *Foxg1* (F,G), *Otx2* (H,I) and *Foxa2* (J,K) in control and *dsSmad1*-transfected+Cerberus-injected embryos. Note the significant rescue of the gene expression in the developing forebrain after Cerberus injection. (L) Model of interactions adapted from Shimamura and Rubenstein (Shimamura and Rubenstein, 1997) suggesting a direct induction of *Foxg1* in the neuroepithelium by Fgf8 from the ANR. (M) Proposed model for the regulation of *Foxg1* expression by the FNC cells. For clarity, anatomical structures are on the left and interactions are on the right. Fgf8 from the ANR interacts with *Smad1* in FNC cells, which controls *Dkk1* expression, acting upstream of *Noggin* and *Gremlin* for the induction of *Foxg1* expression in the telencephalon. *Foxg1* expression maintains the balance between *Otx2* and *Foxa2*. *Dkk1* also controls Cerberus activity in the retroocular region, which regulates *Otx2* and *Foxa2* expression in the di/mesencephalon. Positive and negative regulations are indicated with solid and dashed lines, respectively. Regulations originating from the neuroepithelium are in dark blue; regulations by the FNC cells are in red. ANR, anterior neural ridge; AP, alar plate; BP, basal plate; Di, diencephalon; FNC, facial neural crest; Grem, Gremlin; Mes, mesencephalon; Nogg, Noggin; not, notochord; pcp, pre-chordal plate; Pro, prosencephalon; Rh, rhombencephalon; Tel, telencephalon.

Regulation of *Cerberus* expression by *Dkk1* is required for *Otx2* and *Foxa2* expression

In *Smad1*-depleted embryos, the activity of *Cerberus*, which is known to interfere with Bmp and Wnt signalling (Bouwmeester et al., 1996), was examined at 26ss; its transcripts are normally accumulated in FNC cells that populate the retro- and peri-ocular region (Fig. 8A). After *Smad1* silencing, *Cerberus* activity was totally inhibited (Fig. 8B; n=10). Similarly, when *Dkk1* was over-expressed in FNC cells, the expression of *Cerberus* totally disappeared from the retroocular region (Fig. 8C; n=8). Together, these experiments indicated that *Smad1* expression in FNC impinges on *Dkk1* activity, which, in turn, interferes with *Cerberus* expression.

To see if the loss of *Cerberus* activity can have an effect on brain patterning, we tried to rescue the defects generated by *Smad1* silencing on brain development by injecting Cerberus protein. After electroporation of *dsSmad1* molecules at 4ss (Fig. 8D), we injected a solution of Cerberus recombinant protein (0.1 µg/µl) contrasted with Rhodamine Dextran at 12ss (Fig. 8D,E). Injection was performed bilaterally in a sub-ectodermal location in order to deliver Cerberus protein into the migration routes of FNC cells.

Supplying *dsSmad1*-treated embryos with Cerberus resulted in a potent rescue of the morphological defects: development of the pre-otic vesicles was significantly restored. At 26ss, the expression of *Foxg1* tended to normalise (Fig. 8F,G; n=9). Furthermore, *Otx2* and *Foxa2* expression nearly recovered a normal pattern in the di- and mesencephalon (Fig. 8H-K). Hence, Cerberus activity in FNC cells is required for *Foxg1* regulation in the telencephalon and maintains *Otx2* and *Foxa2* expression at di/mesencephalic level.

DISCUSSION

In this work, we have explored the role of the FNC in brain development by knocking down the expression of a signalling transducer, *Smad1*, which complexes with specific DNA-binding proteins to regulate gene expression. Smad1 belongs to a large family of cytoplasmic mediators for which translocation to the nucleus is triggered by the activity of Tgfβ signalling. *Smad1* expression, strongly detected in the FNC at the neural plate border, declines while FNC cells migrate, then increases in intensity and persists in the FNC-derived mesenchyme populating facial processes until E5.

To investigate the molecular mechanisms by which *Smad1* expression in the FNC affects the developmental programme of cephalic vesicles, we silenced its activity, when its expression is maximal in FNC cell population. dsRNA-driven silencing had efficiently inhibited *Smad1* activity in FNC cells by 1.5 hours following electroporation, and generated conspicuous defects in brain development 24 h later (at 25ss). These defects included microcephaly, which encompasses fore- and midbrain but was particularly pronounced at telencephalic level. The telencephalon dramatically drops to 40% of its normal size. Hemispheres display partial holoprosencephaly, with a vestigial septal region and atrophied choroid plexi. Additionally, *Smad1*-depleted embryos display severe microphtalmia.

These early morphological defects coincide with the downregulation of *Fgf8* in the ANR and the complete loss of *Foxg1* expression in the prosencephalon. *Foxg1* is an early marker of cephalic development, which features the anterior neural plate at gastrula stage in chordates (Merino et al., 1999; Toresson et al., 1998). However, the expansion of its expression to the entire telencephalon is specific to vertebrates.

The effect of ANR in telencephalic specification was first investigated by explants and microsurgical experiments showing the leading role played by this discrete territory in forebrain

Development (2014) 141, 2494-2505 doi:10.1242/dev.101790

specification (Shimamura and Rubenstein, 1997) (Fig. 8L). The morphogenetic action of what was then referred to as the 'prosencephalic organiser' was assigned to the production of *Fgf8* at this level (Shimamura and Rubenstein, 1997; Houart et al., 1998; Shanmugalingam et al., 2000; Storm et al., 2006). The cooperation between *Fgf8* and *Foxg1* allows for the telencephalon to become secondarily specified from the primary prosencephalon (Rubenstein et al., 1998; Rubenstein and Beachy, 1998; Vieira and Martinez, 2006).

The cerebral defects encountered in our *Smad1*-depleted embryos virtually reproduce the anomalies encountered in *Foxg1* mutants (Xuan et al., 1995). However, in *Smad1*-deprived embryos, supplementation with Fgf8 recombinant protein has no effect on *Foxg1* expression and telencephalic development. This indicates that the morphogenetic regulation exerted by FNC cells is crucial for specification of the rostral prosencephalon by stimulation of *Foxg1* expression.

To unravel the involvement of the FNC in the regulation of *Foxg1*, we performed ablation of the ANR at 5ss, before the onset of FNC cell migration: the predictable loss of *Foxg1* expression ensued. By contrast, when mutated forms of Smad1, which mimic the activation of the Fgf8 or Wnt pathways, were transfected into the FNC cells at the time of ANR ablation, a potent rescue of telencephalic development occurred together with restoration of *Foxg1* expression.

Additionally, misregulation of *Foxg1* in the telencephalon was accompanied by perturbations in *Otx2* and *Foxa2* activity in thalamus and tectum, where their expression pattern characterises the alar and basal plate, respectively. *Otx2* is an important marker of dorsal patterning of the fore- and midbrain (Kimura et al., 2001, 2005). Its activity is antagonised by the expression of *Foxa2* in the di/mesencephalic basal plate (Weinstein et al., 1994; Nakano et al., 2000).

In the absence of the FNC, a considerable expansion of *Shh* expression occurs along with a conspicuous ventralisation of the cephalic neuroepithelium (Creuzet et al., 2004). Similarly in the present experiments, *Smad1* silencing also results in a potent ventralisation of the pre-otic brain, as attested by the thickening of the ventral structures at E8. This early phenotype coincides with the lateral expansion of *Foxa2* at the expense of *Otx2* expression, dorsally. Surprisingly, the domain of *Shh* expression remains unchanged whatever the experimental conditions examined. Hence, *Smad1* depletion in FNC decouples *Foxa2* and *Shh* expression in the di- and mesencephalic floor plate, and unmasks the divergent regulation of these two 'basal' markers.

Compared with the phenotype of *dsSmad1*-treated embryos, the outcome of cerebral structures in *Foxg1*-depleted embryos was similar, indicating that the molecular changes in *Otx2* and *Foxa2* primarily stem from the downregulation of *Foxg1*. So, our data uncover an unappreciated role of *Foxg1* in the patterning of the thalamus and tectum through the regulation of *Otx2* and *Foxa2*. These observations reveal that these two genes are subjected to regulation by the telencephalic neuroepithelium. The loss of *Foxg1* function in the telencephalon prejudices the relationship between *Otx2* and *Foxa2* expression, hence reproducing the effects of *Smad1* silencing in FNC cells.

In humans, mutations in *FOXG1* are causally linked to microcephaly and mental retardation, regression of language and manual skills, in atypical Rett and 14q12 microdeletion syndromes (Papa et al., 2008; Allou et al., 2012). But, the cerebral phenotype resulting from *Smad1* silencing in the FNC is also evocative of the deficits encountered in septo-ocula dysplasia (de Morsier, 1956). This syndrome may be caused by heterozygous mutations of *OTX2* (Ragge et al., 2005). Under this condition, syndromic phenotypes encompass severe microphtalmia and cerebral midline defects; these include agenesis of the septum and/or corpus callosum, which together lead to cortical malformations and intellectual deficits. Therefore, our results suggest that atypical Rett syndromes and some related disorders, which involve misregulations of *FOXG1* and *OTX2*, could be neurocristopathic in origin. The overlapping spectrum of cephalic defects encountered in these congenital disorders hints at convergent mechanisms responsible for the clinical pictures of these syndromes and their variant forms. However, the rationale accounting for the shared defects generated by different mutations remain unknown. Here, we show that the FNC exerts a key role in controlling the telencephalic expression of *Foxg1*, which then impinges on *Otx2* activity in the pros- and mesencephalon. Our data put forward an ontogenic scenario, which sheds a new light on the molecular control of these transcription factors by the FNC (Fig. 8M). By building up a network of patterning interactions between the FNC and the developing brain, this study may open new avenues for understanding the aetiology of related intellectual deficits in the light of FNC dysfunctions.

MATERIALS AND METHODS

Avian embryos and surgical procedures

Chick embryos used as a model throughout this study were staged according the number of somite pairs (ss). Experiments were performed either at 4ss for *in ovo* electroporation of premigratory FNC cells, at the 5- to 6-somite stage for ANR ablation or at 10ss for Cerberus protein supplementation. Ablation of the ANR was achieved by using glass micro-scalpels, and was performed either alone or immediately after FNC electroporation. The limit of excision was defined according to the fate map of the cephalic NF (Couly and Le Douarin, 1985, 1987).

In ovo electroporation

Electroporation was achieved using a triple electrode system placed on the vitelline membrane with the two cathodes flanking the developing head with a gap of 5 mm, and the anode facing the anterior neuropore (Creuzet et al., 2002). Before electroporation, nucleic acids were contrasted with a solution of 0.01% Fast Green FCF (Sigma) to control the site of injection, then headed for the targeted tissues by a series of five square pulses of 27 V (T830 BTX, Genetronics). After electroporation, eggs were sealed and incubated at 38°C until reaching the stage required for analysis.

Nucleic acid preparation

Gene silencing was performed by electroporating dsRNA. In mammals, dsRNA yields a non-specific blockade of protein synthesis (Billy et al., 2001; Elbashir et al., 2001). However, in chick, no such effects were ever detected; dsRNA electroporation resulted in highly specific gene inactivation (Pekarik et al., 2003; Stoeckli, 2003). For each series, efficacy of the silencing was analysed by *in situ* hybridisation, RT-PCR and qRT-PCR.

Sense and antisense strands of RNA were synthesised from the cDNA encoding for the targeted gene (Pekarik et al., 2003). After elimination of the cDNA template, single strands were purified and annealed for 5 min at 95°C. dsRNA against *Smad1*, *Foxg1*, *Noggin* and *Gremlin* (Gont and Lough, 2000; Bardot et al., 2001; Li and Vogt, 1993; Osorio et al., 2009) were used at 0.33 µg/µl, 0.4 µg/µl, 0.25 µg/µl and 0.25 µg/µl, respectively. In the control series, solutions of non-annealed sense and anti-sense RNA strands of the targeted genes were transfected at the same concentration as in the experimental series.

For gain-of-function experiments, the following plasmid and RCAS constructs were used: pCAGGS-GFP (Momose et al., 1999), *hSmad1* (human *SMAD1* wild type) at 1.1 µg/µl, *hSmad1*-MM (human *SMAD1* mutated in the three MAPK sites of the linker region) at 1.25 µg/µl, *hSmad1*-GM (human *SMAD1* mutated in the four Gsk3 sites of the linker region) at 1.25 µg/µl (Fuentealba et al., 2007), *Dkk1*-RCAS at 1.1 µg/µl (Chang et al., 2004), *Gremlin*- and *Noggin*-RCAS at 1 µg/µl (Creuzet, 2009). RCAS constructs used in this study allow for the overexpression of the insert but do not produce viral particles. The ectopic gene activity is therefore restricted to the FNC cells and their progenies.

Development (2014) 141, 2494-2505 doi:10.1242/dev.101790

Supplementation with recombinant proteins

Depending on the series, protein supplementation of *dsSmad1*-electroporated embryos was delivered by either injecting a solution or implanting soaked beads. A solution of Cerberus protein (0.100 µg/µl in PBS; R&D Systems) contrasted with 0.01% Rhodamine Dextran (Sigma) was bilaterally injected into the migration routes of FNC cells, adjacent to the di- and mesencephalic vesicles. For Fgf8 supplementation, beads were soaked in a solution of Fgf8 recombinant protein (0.125 µg/µl; R&D Systems) overnight at 4°C, then bilaterally implanted in contact with the ANR. This concentration has been shown to induce a potent rescue of head and brain development after FNC ablation (Creuzet et al., 2004).

In situ hybridisation

Whole-mount *in situ* hybridisations (Creuzet et al., 2006) were performed using the following probes: *Bmp4* (Francis et al., 1994), *Cerberus* (provided by Dr Ricardo Garcez, Institut de Neurobiologie, France), *Smad1*, *Smad5* (Gont and Lough, 2000), *Foxg1* (Chapman et al., 2002), *Six3* (Geng et al., 2008), *Pax6* (Walther and Gruss, 1991), *Foxa2* (Ruiz i Altaba et al., 1995), *Fgf8* (Crossley et al., 1996), *Gremlin*, *Noggin* (Connolly et al., 1997), *Otx2* (Boncinelli et al., 1993), *Shh* (Riddle et al., 1993), *Wnt1*, *Wnt3a* (Hollyday et al., 1995), *Wnt8b* (Garcia-Lopez et al., 2004).

Whole-mount staining and immunocytochemistry

FNC cell migration and cell proliferation were demonstrated by immunocytochemistry with monoclonal antibodies against HNK1 (CD57; Santa Cruz Biotechnology) and pH3 (Sigma), and detected with Alexa Fluor 488- and Alexa Fluor-594-labelled secondary antibodies (Life Technology, Invitrogen). Cell death was detected by Lysotracker Red (LTR; Invitrogen) staining prior to fixation (Garcez et al., 2014). Quantification of cell proliferation and death was performed on vibratome sections using ImageJ software.

Histology

Embryos were fixed in a solution of 60% ethanol, 30% formaldehyde (37%, stock solution) and 10% acetic acid (100%, stock solution), for 24 h, dehydrated in ethanol, permeabilised in toluene and embedded in paraffin. Cresyl Violet staining was performed on 7-µm-thick sections.

RT-PCR analysis and *Dkk1* probe construction

Total RNA was isolated from 25ss pre-otic heads in Trizol Reagent (Invitrogen). cDNA was obtained with MMLV reverse transcriptase (Invitrogen) and oligodT12-18 primers. Amplification was performed from 1 µg cDNA, using specific primer pairs for *Fgf8* (For: ccctgctcctcgctcttcag; Rev: ctcctgcggttgaaggggta), *Foxg1* (For: ctccgtgaacctcctggcgg; Rev: ggccctggccgtcatcgaag), *Otx2* (For: accaaaccgcctcctggaagt; Rev: cccacgggccttcacaaaaacct), *Foxa2* (For: ccctgctggctccaggtggt; Rev: aaggcaaaccgaggggaccg), *Noggin* (For: agctgcgcaggaagctgcag; Rev: acgtaccggggccaaaagcg), *Dkk1* (For: gcacacttgccagcggcact; Rev: ctcccacgagcggggctaga), *Dkk2* (For: aggtgatccctgcctgcggt; Rev: agcaggcacagccattgtggaa) and *Dkk3* (For: gcgctgatggaggacacgca; Rev: tgcacatgggcagcgctcta).

Quantitative real-time PCR (qRT-PCR) analysis of gene expression

Quantifications were performed on seven control, six *dsSmad1*-treated and seven rescued embryos. Primer pairs (Invitrogen) were designed specifically for each gene: *Smad1* (For: aacatgatggcacccggaat; Rev: gatgctggtggaagaggcat), *Fgf8* (For: gtacgagggctggtacatgg; Rev: cggttgaaggggtagttgag), *Foxg1* (For: caacgcgctcatcatgatgg; Rev: ttgagagagaggttgtggcg), *Otx2* (For: acccaggcatcaggttacag; Rev: gaggctggagactggttgag), *Foxa2* (For: ccttctaccgccagaaccag; Rev: caaacatgttgcccgagtcg), *Pax6* (For: tcagcacaagcgtttaccag; Rev: ggttgcataggcaggttgtt), *Wnt1* (For: aaatgggcactgggtgtct; Rev: cctcgagggtcatctacgg), *Wnt3a* (For: ggagatcatgcccagcgtag; Rev: gcggattccctggtagcttt), *Wnt8b* (For: gaactgcagcctgggagatt; Rev: tctccagggcatccacaaac) and *Dkk1* (For: ccggagcagaaggttgtttc; Rev: gtaccacgtcccagtcctg). Quantitative PCR reactions were performed using LightCycler (Roche), and sample analysis was carried out in triplicate. Ct values were obtained by using Promega software (v.2.0.4) and relative quantifications (ΔΔCt) normalised to *Gapdh* gene activity. Statistical analyses were performed with the GraphPad Prism5.0 software assuming a confidence interval of 95%, and compared using the non-parametric Mann–Whitney U-test.

Morphometric analysis

Brain growth was estimated on E4 embryos by measuring the distance from the optic stalk to the top of each cephalic vesicle: telencephalon, thalamus and optic tectum. Data from control, *dsSmad1*-electroporated and *dsSmad1*/*hSmad1*-co-transfected embryos were compared using one-way ANOVA and analysed with the GraphPad Prism 4.0 software.

Acknowledgements

The authors thank Profs Le Douarin and Moura Neto for their support, advices and critical reading of the manuscript and to Prof. De Robertis for kindly providing *Smad* constructs. They also thank Drs Chapman, Kiecker, Lough and Widelitz for providing plasmids.

Competing interests

The authors declare no competing financial interests.

Author contributions

D.P.A. performed experiments and data analysis, and prepared the manuscript; S.G. performed experiments and data analysis; S.C. developed concepts and approaches, performed experiments and data analysis, and prepared the manuscript.

Funding

D.P.A. held fellowships from CAPES-College Doctoral Franco-Brésilien, Fondation des Treilles and Institut Necker Paris. This work was supported by the Centre National de la Recherche Scientifique (CNRS), and grants from the National Funding Agency for Research (ANR) [ANR-Blan-0153], Soutien à l'Encadrement de Thèse en Cotutelle (SETCI) (Ile-de-France) and Association Française du Syndrome de Rett (AFSR) [2012-05].

References

Acampora, D., Avantaggiato, V., Tuorto, F., Briata, P., Corte, G. and Simeone, A. (1998). Visceral endoderm-restricted translation of *Otx1* mediates recovery of *Otx2* requirements for specification of anterior neural plate and normal gastrulation. *Development* **125**, 5091-5104.

Allou, L., Lambert, L., Amsallem, D., Bieth, E., Edery, P., Destrée, A., Rivier, F., Amor, D., Thompson, E., Nicholl, J. et al. (2012). 14q12 and severe Rett-like phenotypes: new clinical insights and physical mapping of FOXG1 regulatory elements. *Eur. J. Hum. Genet.* **20**, 1216-1223.

Anderson, R. M., Lawrence, A. R., Stottmann, R. W., Bachiller, D. and Klingensmith, J. (2002). Chordin and noggin promote organizing centers of forebrain development in the mouse. *Development* **129**, 4975-4987.

Ang, S. L., Jin, O., Rhinn, M., Daigle, N., Stevenson, L. and Rossant, J. (1996). A targeted mouse Otx2 mutation leads to severe defects in gastrulation and formation of axial mesoderm and to deletion of rostral brain. *Development* **122**, 243-252.

Bardot, B., Lecoin, L., Huillard, E., Calothy, G. and Marx, M. (2001). Expression pattern of the drm/gremlin gene during chicken embryonic development. *Mech. Dev.* **101**, 263-265.

Billy, E., Brondani, V., Zhang, H., Müller, U. and Filipowicz, W. (2001). Specific interference with gene expression induced by long, double-stranded RNA in mouse embryonal teratocarcinoma cell lines. *Proc. Natl. Acad. Sci. U.S.A.* **98**, 14428-14433.

Boncinelli, E., Gulisano, M. and Broccoli, V. (1993). Emx and Otx homeobox genes in the developing mouse brain. *J. Neurobiol.* **24**, 1356-1366.

Bouwmeester, T., Kim, S. H., Sasai, Y., Lu, B. and De Robertis, E. M. (1996). Cerberus is a head-inducing secreted factor expressed in the anterior endoderm of Spemann's organizer. *Nature* **382**, 595-601.

Braun, M. M., Etheridge, A., Bernard, A., Robertson, C. P. and Roelink, H. (2003). Wnt signaling is required at distinct stages of development for the induction of the posterior forebrain. *Development* **130**, 5579-5587.

Chang, C.-H., Jiang, T.-X., Lin, C.-M., Burrus, L. W., Chuong, C.-M. and Widelitz, R. (2004). Distinct Wnt members regulate the hierarchical morphogenesis of skin regions (spinal tract) and individual feathers. *Mech. Dev.* **121**, 157-171.

Chapman, S. C., Schubert, F. R., Schoenwolf, G. C. and Lumsden, A. (2002). Analysis of spatial and temporal gene expression patterns in blastula and gastrula stage chick embryos. *Dev. Biol.* **245**, 187-199.

Connolly, D. J., Patel, K. and Cooke, J. (1997). Chick noggin is expressed in the organizer and neural plate during axial development, but offers no evidence of involvement in primary axis formation. *Int. J. Dev. Biol.* **41**, 389-396.

Couly, G. F. and Le Douarin, N. M. (1985). Mapping of the early neural primordium in quail-chick chimeras. I. Developmental relationships between placodes, facial ectoderm, and prosencephalon. *Dev. Biol.* **110**, 422-439.

Couly, G. F. and Le Douarin, N. M. (1987). Mapping of the early neural primordium in quail-chick chimeras. II. The prosencephalic neural plate and neural folds: implications for the genesis of cephalic human congenital abnormalities. *Dev. Biol.* **120**, 198-214.
Creuzet, S. E. (2009). Regulation of pre-otic brain development by the cephalic neural crest. *Proc. Natl. Acad. Sci. U.S.A.* **106**, 15774-15779.
Creuzet, S., Couly, G., Vincent, C. and Le Douarin, N. M. (2002). Negative effect of Hox gene expression on the development of the neural crest-derived facial skeleton. *Development* **129**, 4301-4313.
Creuzet, S., Schuler, B., Couly, G. and Le Douarin, N. M. (2004). Reciprocal relationships between Fgf8 and neural crest cells in facial and forebrain development. *Proc. Natl. Acad. Sci. U.S.A.* **101**, 4843-4847.
Creuzet, S. E., Martinez, S. and Le Douarin, N. M. (2006). The cephalic neural crest exerts a critical effect on forebrain and midbrain development. *Proc. Natl. Acad. Sci. U.S.A.* **103**, 14033-14038.
Crossley, P. H., Minowada, G., MacArthur, C. A. and Martin, G. R. (1996). Roles for FGF8 in the induction, initiation, and maintenance of chick limb development. *Cell* **84**, 127-136.
Danesin, C., Peres, J. N., Johansson, M., Snowden, V., Cording, A., Papalopulu, N. and Houart, C. (2009). Integration of telencephalic Wnt and hedgehog signaling center activities by Foxg1. *Dev. Cell* **16**, 576-587.
de Morsier, G. (1956). Études sur les dysraphies, crânioencéphaliques. III. Agénésie du septum pelludicum avec malformation du tractus optique. La dysplasie septo-optique. *Schweiz. Arch. Neurol. Psychiatr.* **77**, 267-292.
Echevarría, D., Vieira, C., Gimeno, L. and Martínez, S. (2003). Neuroepithelial secondary organizers and cell fate specification in the developing brain. *Brain. Res. Rev.* **43**, 179-191.
Elbashir, S. M., Harborth, J., Lendeckel, W., Yalcin, A., Weber, K. and Tuschl, T. (2001). Duplexes of 21-nucleotide RNAs mediate RNA interference in cultured mammalian cells. *Nature* **411**, 494-498.
Erter, C. E., Wilm, T. P., Basler, N., Wright, C. V. and Solnica-Krezel, L. (2001). Wnt8 is required in lateral mesendodermal precursors for neural posteriorization in vivo. *Development* **128**, 3571-3583.
Francis, P. H., Richardson, M. K., Brickell, P. M. and Tickle, C. (1994). Bone morphogenetic proteins and a signalling pathway that controls patterning in the developing chick limb. *Development* **120**, 209-218.
Fuentealba, L. C., Eivers, E., Ikeda, A., Hurtado, C., Kuroda, H., Pera, E. M. and De Robertis, E. M. (2007). Integrating patterning signals: Wnt/GSK3 regulates the duration of the BMP/Smad1 signal. *Cell* **131**, 980-993.
Garcez, R. C., Le Douarin, N. M. and Creuzet, S. E. (2014). Combinatorial activity of *Six1*-2-4 genes in cephalic neural crest cells controls craniofacial and brain development. *Cell. Mol. Life. Sci.* **71**, 2149-2164.
Garcia-Lopez, R., Vieira, C., Echevarria, D. and Martinez, S. (2004). Fate map of the diencephalon and the zona limitans at the 10-somites stage in chick embryos. *Dev. Biol.* **268**, 514-530.
Geng, X., Speirs, C., Lagutin, O., Inbal, A., Liu, W., Solnica-Krezel, L., Jeong, Y., Epstein, D. J. and Oliver, G. (2008). Haploinsufficiency of Six3 fails to activate Sonic hedgehog expression in the ventral forebrain and causes holoprosencephaly. *Dev. Cell.* **15**, 236-247.
Gont, L. and Lough, J. (2000). Differential expression of cSmad1 and cSmad5 in the primitive streak during chick embryo gastrulation. *Anat. Rec.* **260**, 102-105.
Hanashima, C., Li, S. C., Shen, L., Lai, E. and Fishell, G. (2004). Foxg1 suppresses early cortical cell fate. *Science* **303**, 56-59.
Hoch, R. V., Rubenstein, J. L. and Pleasure, S. (2009). Genes and signaling events that establish regional patterning of the mammalian forebrain. *Semin. Cell Dev. Biol.* **20**, 378-386.
Hollyday, M., McMahon, J. A. and McMahon, A. P. (1995). Wnt expression patterns in chick embryo nervous system. *Mech. Dev.* **52**, 9-25.
Houart, C., Westerfield, M. and Wilson, S. W. (1998). A small population of anterior cells patterns the forebrain during zebrafish gastrulation. *Nature* **391**, 788-792.
Kim, A. S., Lowenstein, D. H. and Pleasure, S. J. (2001). Wnt receptors and Wnt inhibitors are expressed in gradients in the developing telencephalon. *Mech. Dev.* **103**, 167-172.
Kimura, C., Shen, M. M., Takeda, N., Aizawa, S. and Matsuo, I. (2001). Complementary functions of Otx2 and Cripto in initial patterning of mouse epiblast. *Dev. Biol.* **235**, 12-32.
Kimura, J., Suda, Y., Kurokawa, D., Hossain, Z. M., Nakamura, M., Takahashi, M., Hara, A. and Aizawa, S. (2005). Emx2 and Pax6 function in cooperation with Otx2 and Otx1 to develop caudal forebrain primordium that includes future archipallium. *J. Neurosci.* **25**, 5097-5108.
Le Douarin, N. M., Couly, G. and Creuzet, S. E. (2012). The neural crest is a powerful regulator of pre-otic brain development. *Dev. Biol.* **366**, 74-82.
Li, J. and Vogt, P. K. (1993). The retroviral oncogene qin belongs to the transcription factor family that includes the homeotic gene fork head. *Proc. Natl. Acad. Sci. U.S.A.* **90**, 4490-4494.
Manuel, M., Martynoga, B., Yu, T., West, J. D., Mason, J. O. and Price, D. J. (2010). The transcription factor Foxg1 regulates the competence of telencephalic cells to adopt subpallial fates in mice. *Development* **137**, 487-497.
Martynoga, B., Morrison, H., Price, D. J. and Mason, J. O. (2005). Foxg1 is required for specification of ventral telencephalon and region-specific regulation of dorsal telencephalic precursor proliferation and apoptosis. *Dev. Biol.* **283**, 113-127.
McMahon, A. P. and Bradley, A. (1990). The Wnt-1 (int-1) proto-oncogene is required for development of a large region of the mouse brain. *Cell* **62**, 1073-1085.
Merino, R., Rodriguez-Leon, J., Macias, D., Ganan, Y., Economides, N. A. and Hurle, J. M. (1999). The BMP antagonist Gremlin regulates outgrowth, chondrogenesis and programmed cell death in the developing limb. *Development* **126**, 5515-5522.
Momose, T., Tonegawa, A., Takeuchi, J., Ogawa, H., Umesono, K. and Yasuda, K. (1999). Efficient targeting of gene expression in chick embryos by microelectroporation. *Dev. Growth. Differ.* **41**, 335-344.
Mukhopadhyay, M., Shtrom, S., Rodriguez-Esteban, C., Chen, L., Tsukui, T., Gomer, L., Dorward, D. W., Glinka, A., Grinberg, A., Huang, S. P. et al. (2001). Dickkopf1 is required for embryonic head induction and limb morphogenesis in the mouse. *Dev. Cell.* **1**, 423-434.
Nakano, T., Murata, T., Matsuo, I. and Aizawa, S. (2000). OTX2 directly interacts with LIM1 and HNF-3beta. *Biochem. Biophys. Res. Commun.* **267**, 64-70.
Osorio, L., Teillet, M.-A. and Catala, M. (2009). Role of noggin as an upstream signal in the lack of neuronal derivatives found in the avian caudal-most neural crest. *Development* **136**, 1717-1726.
Papa, F. T., Mencarelli, M. A., Caselli, R., Katzaki, E., Sampieri, K., Meloni, I., Ariani, F., Longo, I., Maggio, A., Balestri, P. et al. (2008). A 3 Mb deletion in 14q12 causes severe mental retardation, mild facial dysmorphisms and Rett-like features. *Am. J. Med. Genet. A.* **146**, 1994-1998.
Pekarik, V., Bourikas, D., Miglino, N., Joset, P., Preiswerk, S. and Stoeckli, E. T. (2003). Screening for gene function in chicken embryo using RNAi and electroporation. *Nat. Biotechnol.* **21**, 93-96.
Plouhinec, J. L., Leconte, L., Sauka-Spengler, T., Bovolenta, P., Mazan, S. and Saule, S. (2005). Comparative analysis of gnathostome Otx gene expression patterns in the developing eye: implications for the functional evolution of the multigene family. *Dev. Biol.* **278**, 560-575.
Ragge, N. K., Brown, A. G., Poloschek, C. M., Lorenz, B., Henderson, R. A., Clarke, M. P., Russell-Eggitt, I., Fielder, A., Gerrelli, D., Martinez-Barbera, J. P. et al. (2005). Heterozygous mutations of OTX2 cause severe ocular malformations. *Am. J. Hum. Genet.* **76**, 1008-1022.
Riddle, R. D., Johnson, R. L., Laufer, E. and Tabin, C. (1993). Sonic hedgehog mediates the polarizing activity of the ZPA. *Cell* **75**, 1401-1416.
Rubenstein, J. L. R. and Beachy, P. A. (1998). Patterning of the embryonic forebrain. *Curr. Opin. Neurobiol.* **8**, 18-26.
Rubenstein, J. L.R., Shimamura, K., Martinez, S. and Puelles, L. (1998). Regionalization of the prosencephalic neural plate. *Annu. Rev. Neurosci.* **21**, 445-477.
Ruiz i Altaba, A., Placzek, M., Baldassare, M., Dodd, J. and Jessell, T. M. (1995). Early stages of notochord and floor plate development in the chick embryo defined by normal and induced expression of HNF-3 beta. *Dev. Biol.* **170**, 299-313.
Shanmugalingam, S., Houart, C., Picker, A., Reifers, F., MacDonald, R., Barth, A., Griffin, K., Brand, M. and Wilson, S. W. (2000). Ace/Fgf8 is required for forebrain commissure formation and patterning of the telencephalon. *Development* **127**, 2549-2561.
Shimamura, K. and Rubenstein, J. L. (1997). Inductive interactions direct early regionalization of the mouse forebrain. *Development* **124**, 2709-2718.
Stoeckli, E. T. (2003). RNAi in avian embryos. In *RNAi: A Guide to Gene Silencing* (ed. **G. J. Hannon**), pp. 297-312. New-York: Cold Spring Harbor Laboratory.
Storm, E. E., Garel, S., Borello, U., Hebert, J. M., Martinez, S., McConnell, S. K., Martin, G. R. and Rubenstein, J. L. R. (2006). Dose-dependent functions of Fgf8 in regulating telencephalic patterning centers. *Development* **133**, 1831-1844.
Tao, W. and Lai, E. (1992). Telencephalon-restricted expression of BF-1, a new member of the HNF-3/fork head gene family, in the developing rat brain. *Neuron* **8**, 957-966.
Toresson, H., Martinez-Barbera, J. P., Bardsley, A., Caubit, X. and Krauss, S. (1998). Conservation of BF-1 expression in amphioxus and zebrafish suggests evolutionary ancestry of anterior cell types that contribute to the vertebrate telencephalon. *Dev. Genes. Evol.* **208**, 431-439.
Tzahor, E., Kempf, H., Mootoosamy, R. C., Poon, A. C., Abzhanov, A., Tabin, C. J., Dietrich, S. and Lassar, A. B. (2003). Antagonists of Wnt and BMP signalling promote the formation of vertebrate head muscle. *Genes. Dev.* **17**, 3087-3099.
Vieira, C. and Martinez, S. (2006). Sonic hedgehog from the basal plate and the zona limitans intrathalamica exhibits differential activity on diencephalic molecular regionalization and nuclear structure. *Neuroscience* **143**, 129-140.
Vieira, C., Pombero, A., Garcia-Lopez, R., Gimeno, L., Echevarria, D. and Martinez, S. (2010). Molecular mechanisms controlling brain development: an overview of neuroepithelial secondary organizers. *Int. J. Dev. Biol.* **54**, 7-20.
Walther, C. and Gruss, P. (1991). Pax-6, a murine paired box gene, is expressed in the developing CNS. *Development* **113**, 1435-1449.
Weinstein, D. C., Ruiz i Altaba, A., Chen, W. S., Hoodless, P., Prezioso, V. R., Jessell, T. M. and Darnell, J. E., Jr (1994). The winged-helix transcription factor HNF-3 beta is required for notochord development in the mouse embryo. *Cell* **78**, 575-588.
Xuan, S., Baptista, C. A., Balas, G., Tao, W., Soares, V. C. and Lai, E. (1995). Winged helix transcription factor BF-1 is essential for the development of the cerebral hemispheres. *Neuron* **14**, 1141-1152.